

Spatial-temporal distribution of atmospheric temperature anomalies connected with seismic activity in Tien-Shan

L. G. SVERDLIK and S. A. IMASHEV

Research Station of the Russian Academy of Sciences, Bishkek – 720 049, Kyrgyzstan

(Received 22 May 2019, Accepted 23 May 2020)

e mail : l.sverdlik@mail.ru

सार – इस शोध पत्र में हमने उत्तरी और मध्य टीएन-शान के ऊपर ऊपरी क्षोभ मंडल/निम्न समताप मंडल (UTLS) में उपग्रह रिमोट सेंसिंग से प्राप्त किए गए स्थानिक-कालिक तापमान में हुए परिवर्तनों का विश्लेषण किया है जिनकी तुलना (1992 से 2015 तक) भूकंपीय गतिविधि से की गई है। तापमान समय श्रृंखला में इन असंगत परिवर्तनों को पूर्व-भूकंपीय संकेतकों के रूप में उपयोग किया गया था। असंगत भिन्नता मापदंडों की गणना क्षोभमंडलीय सीमा द्वारा अलग किए गए UTLS समदाबी स्तरों पर आयाम और कम समय के तापमान विविधताओं के चरणों के लिए की जाती है। परिणाम बताते हैं कि UTLS के क्षेत्र में स्थानिक संरचना और तापमान विसंगतियों की गतिशीलता का भूकंपीय गतिविधि के साथ पर्याप्त स्थाई संबंध होता है। हमने $M_{5.0}$ के परिमाण के 12 शक्तिशाली भूकंपों के आधार पर स्थानिक और समय परिवर्तनशीलता में हुई तापमान विसंगति का आकलन किया है। मुख्य भूकंपीय घटना के लगभग 3 से 72 घंटे पहले के सभी मामलों में तापमान विसंगतियां देखी गई हैं।

ABSTRACT. In this paper we analyzed spatial-temporal temperature changes in the upper troposphere/lower stratosphere (UTLS) above the Northern and Central Tien-Shan detected by satellite remote sensing which have been compared against seismic activity in (1992-2015). These anomalous changes in temperature time series were used as pre-seismic indicators. Anomalous variation parameters were calculated accounting for amplitude and phase of short-time temperature variations at UTLS isobaric levels separated by the tropopause. The results show that the spatial structure and dynamics of temperature anomalies in the area of UTLS have a sufficiently stable relation to seismic activity. We estimated the spatial and time variability of anomalous temperature perturbations on the basis of 12 strongest earthquakes with magnitudes $M_{5.0}$. The temperature anomalies were observed in all considered cases from ~3 to 72 hours before the main seismic event.

Key words – Earthquake, Satellite data, Upper troposphere, Lower stratosphere, Temperature anomalies, Tropopause.

1. Introduction

Study of strong earthquakes impacting the atmospheric parameters have a long history with active period during the last decades due to substantial progress in the development and improvement of satellite technologies, as well as accessibility of a great number of dedicated services and databases (Tronin, 2010; Pulinetes *et al.*, 2014; Prakash and Srivastava, 2015; Yadav and Pathak, 2018; Jiao *et al.*, 2018; Ouzounov *et al.*, 2019).

Temperature measurements are of great importance for studying the atmospheric effects of earthquakes. It is the key parameter, which defines dynamic processes and structural changes of atmosphere. The atmospheric thermal stratification has a strongly pronounced layered (by the rate of temperature change or gradient γ) nature. The tropopause inversion layer (TIL) separating

the convectively mixed troposphere ($\gamma < 0$) from the more stable and stratified stratosphere (usually $\gamma > 0$) is characterized by great dynamic variability and sensitivity to various perturbations and atmospheric wave activity (Pilch *et al.*, 2017). Circulation processes of planetary and synoptic scale, primarily related to cyclone and anticyclone passing (Randel *et al.*, 2007), change in the solar activity and stratospheric ozone content (Morozova *et al.*, 2017), radiation processes and mass exchange between the troposphere and the stratosphere (Birner, 2006; Manney *et al.*, 2017) play an important role in UTLS temperature variations modulations. In addition, retrospective analysis of satellite during the catastrophic earthquake in Fukushima, Japan, in 2011 showed that the strongest negative correlation between temperature changes at isobaric levels separated by the tropopause coincided with a period of high seismic activity (Kashkin *et al.*, 2012; Kashkin, 2013).

TABLE 1
Earthquakes parameters ($M \geq 5.0$)

No.	Date	Time	Latitude ($^{\circ}$ N)	Longitude ($^{\circ}$ E)	Depth (km)	M	N
EQ01	19 Aug 1992	02:04:36	42.07	73.63	20.0	7.4	89
EQ02	16 Jan 2004	09:06:18	42.55	75.30	14.0	6.0	14
EQ03	25 Dec 2006	20:00:58	42.11	76.03	0.8	6.7	20
EQ04	08 Jan 2007	17:21:49	39.80	70.31	16.0	6.0	2
EQ05	05 Oct 2008	15:52:42	39.53	73.82	27.4	6.7	11
EQ06	19 Jan 2010	17:35:45	42.09	72.09	0.6	5.0	3
EQ07	18 Mar 2011	09:36:27	43.02	74.95	17.1	5.0	2
EQ08	05 Feb 2012	07:10:15	41.40	74.76	10.0	5.6	5
EQ09	11 Mar 2013	03:01:37	40.12	77.47	10.0	5.4	2
EQ10	14 Nov 2014	01:24:16	42.19	77.23	10.1	5.2	1
EQ11	17 Nov 2015	17:29:37	40.43	73.19	3.1	5.6	7
EQ12	07 Dec 2015	08:30:57	41.73	74.61	15.9	5.5	3

* M - magnitude; N - number of seismic events ($M > 2.0$) during the specified 24 hours

However, complex interaction of different-scale processes in UTLS makes it difficult to study the atmospheric response to seismic activity and requires new methods for the processing of experimental data. RST (Robust Satellite Techniques) method was widely applied to detect and localize deviations of parameters from their typical behavior (Tramutoli *et al.*, 2001; Pergola *et al.*, 2010; Zhang and Meng, 2019; Tramutoli *et al.*, 2019). Basic principles of RST method combined with spectral and correlation analysis provide the basis of our algorithm, which, in contrast to conventional methods, is supplemented by a special module for the detection of short-time anomalies in temperature time series. The retrospective analysis of satellite data using the algorithm shows correlation between seismic activity and anomalous temperature variations in UTLS preceding strong seismic events of $M > 6.0$ in the territory of European countries (Sverdlik and Imashev, 2018) and in various Asian regions (Sverdlik *et al.*, 2019; Kashkin *et al.*, 2020). This can indicate a probable relation between strong earthquakes and the observed temperature variations in UTLS.

In this paper we present a modified version of the previously developed (Sverdlik and Imashev, 2019) algorithm, which allows the detection of short-time anomalous variations in the spatial-temporal distribution of temperature. To evaluate our algorithm, we applied it to the analysis of atmospheric effects of earthquakes with magnitude of $M \geq 5.0$, registered in the territory of Kyrgyzstan and near its boundaries.

2. Initial seismic and satellite data

To study temperature variability in pre-seismic, co-seismic and post-seismic periods we chose 12 earthquakes with magnitudes from 5.0 to 7.4, which took place in Kyrgyzstan and nearby territories in 1992-2015. The main characteristics of seismic events in the Northern and Central Tien-Shan presented in the Table 1. We used data from Institute Seismology of Kyrgyzstan and KNET seismology network of Research Station of the Russian Academy of Sciences in Bishkek. Magnitude estimation for the earthquakes is performed according to the following formula : $M = [\lg(E) - 4.8] / 1.5$ (E – seismic wave energy in joules). To obtain data for the seismic events outside of KNET network we used online version of the USGS global catalog (<https://earthquake.usgs.gov/earthquakes/search/>). Locations of the earthquake epicenters are presented in Fig. 1. To assess the sensitivity of the developed algorithm we also analyzed seismic events with magnitudes $4.0 < M < 5.0$. The epicenters of these 58 events are also presented in the map.

To study pre-seismic atmospheric perturbations we used temperature data from the MERRA-2 reanalysis system [<https://disc.gsfc.nasa.gov/datasets>]. Comparison of reanalysis satellite data of MERRA-2 with remote sensing data demonstrated good consistency and quality in spatial structure and UTLS dynamics reconstruction (Manney *et al.*, 2017). This interactive service provides open access to M2I3NPASM Version V5.12.4 data files in the net CDF format. The data represent arrays of

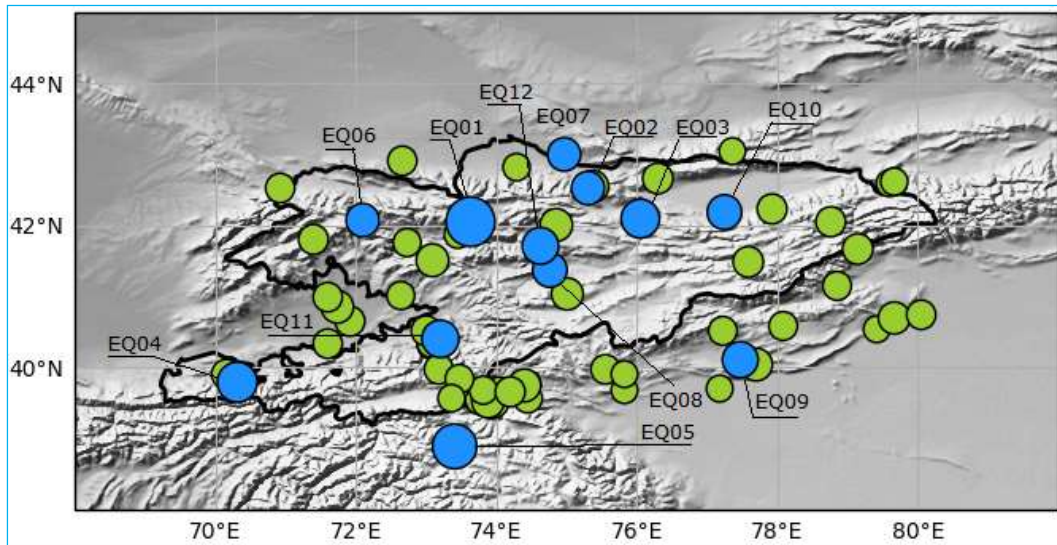


Fig. 1. Earthquake epicenters with magnitudes $M \geq 5.0$ (presented in the Table) and $4.0 < M < 5.0$

synthesized temperature values for each atmospheric level (ASM data type). As an input data for the algorithms, we used atmospheric temperature values at standard isobaric levels from 450 to 70 hPa. The area of interest was $37 - 46^\circ \text{N}$ and $65 - 85^\circ \text{E}$ with the size of the grid $0.5^\circ \times 0.625^\circ$. Resolution of temperature time series $T(t)$ was $\Delta t = 3\text{h}$, providing a sufficiently good detailing of the anomaly formation process.

3. Description of satellite data processing algorithm

Establishing the relation between dynamics of processes in the atmosphere and the lithosphere was based on the assumption that variations of parameters caused by seismic activity differ significantly from background fluctuations that occur during the periods without strong earthquakes. This implies the necessity to identify pre-seismic indicators of abnormal behavior in time series of temperature data. For this purpose, we used integral indexes, which were calculated with regard to variations in temperature amplitude and phase at UTLS levels separated by the tropopause (Sverdlik *et al.*, 2019). The new algorithm make it possible to determine not only temporal, but also spatial distribution of short-time anomalies in temperature; it includes the following stages:

3.1. Preprocessing satellite data

At the first stage, we performed a preliminary processing of satellite data fragments. We prepared time series of $T(t)$ with resolution of $\Delta t = 3\text{h}$, containing temperature values for atmospheric levels (p_k) from 450 to 70 hPa for each seismic event. Length of the analyzed

series was 90 days (45 days before and after the earthquake date).

3.2. Spectral analysis of atmospheric temperature time series

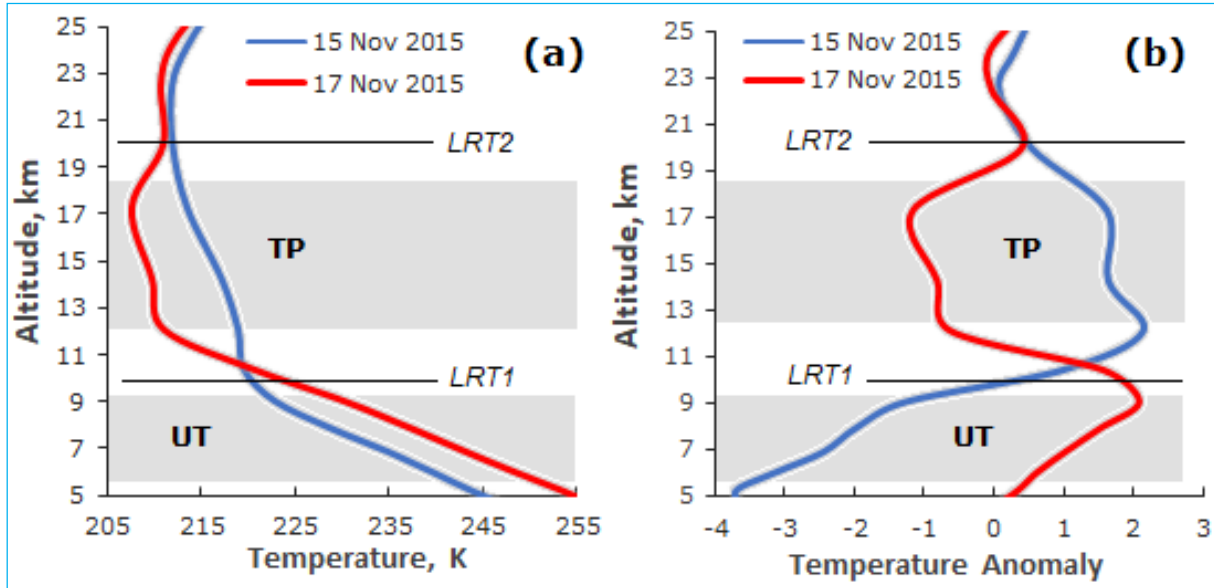
Temperature variations observed in UTLS have components with varying periodicity and amplitude. We used continuous wavelet transform to identify the stationary and non-stationary components in our data. The linear trend and low frequency periodic (seasonal) constituents were excluded from the initial time series.

3.3. Filtration of short-time temperature variations

To retrieve short-time variations we applied nonlinear filtering based on discrete wavelet transform, which has several advantages comparing to moving average or high-order polynomials (Donoho and Johnstone, 1994; Gadre *et al.*, 2014). We consider anomalous change in quasiperiodic components with the period of $\sim 4-6$ days as the main features characterizing atmospheric temperature prior to strong earthquakes (Sanchez-Dulcet *et al.*, 2015; Sverdlik *et al.*, 2019).

3.4. Calculation of atmospheric temperature anomalies

We converted short-time temperature variations at each isobaric level to dimensionless quantity. For this purpose, we retrieve dynamics of temperature anomalies (θT) as deviation of the current temperature value from the average monthly level, normalized to standard deviation :



Figs. 2(a&b). Transformation of vertical profiles of temperature (a) and temperature anomalies (b) in UTLS prior to the earthquake with $M = 5.8$ (17 November, 2015)

$$\Theta T(x, y, n, t, p) = \frac{T(x_i, y_j, n, t, p_k) - \langle T(x_i, y_j, p_k) \rangle}{\sigma_T(x_i, y_j, n, t, p_k)} = \frac{\Delta T(x_i, y_j, n, t, p_k)}{\sigma_T(x_i, y_j, p_k)} \quad (1)$$

where,

- n – the day of measurement;
- t – the time of measurement;
- x_i – altitude;
- y_j – longitude;
- $T(x_i, y_j, n, t, p_k)$ – current temperature value at each isobaric level (p_k);
- $\langle T(x_i, y_j, p_k) \rangle$ – the average temperature;
- $\sigma_T(x_i, y_j, p_k)$ – standard deviation.

3.5. Selection of altitude ranges

At this stage we determined the most informative isobaric levels in UTLS (ΘT_{UT} and ΘT_{TP}), which should be used for particular locations, taking into account local

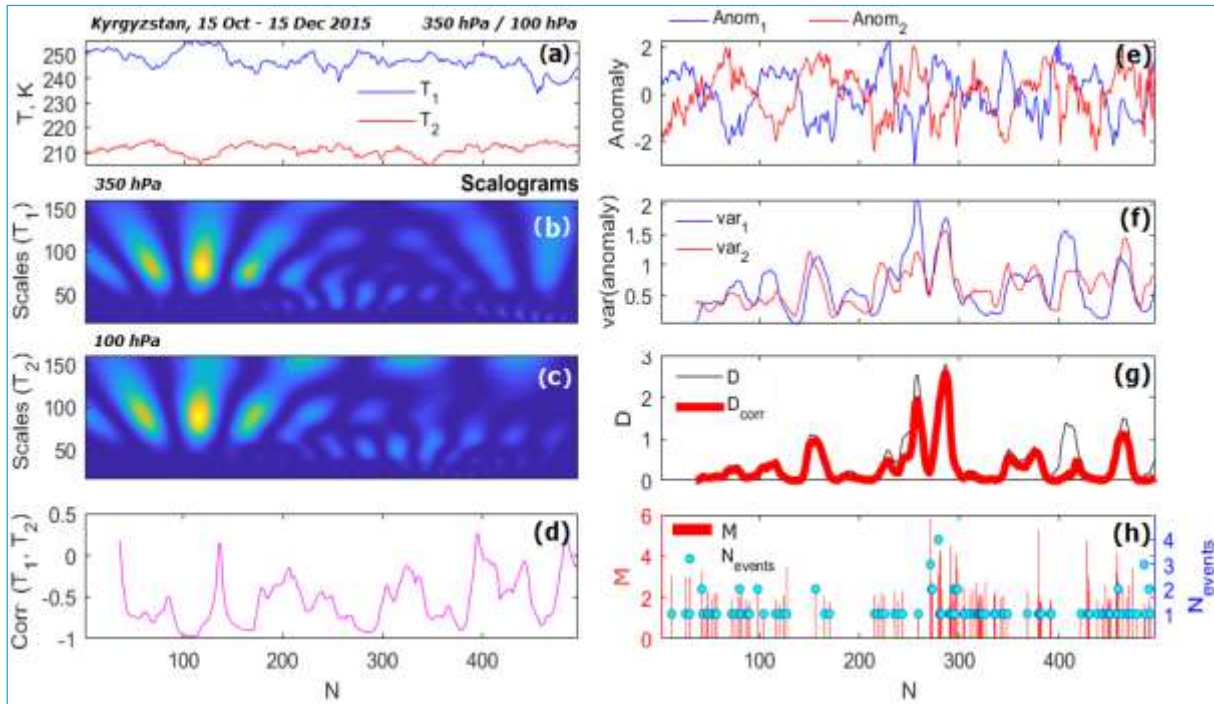
peculiarity in temperature profile. For this purpose, we calculated correlation (R) between temperature variations at each pair of the isobaric levels. Matrix representation of correlation coefficients allows us to select the areas, divided by the tropopause LRT1 (Lapse Rate Tropopause), where the most intensive and antiphase oscillations took place [Figs. 2(a&b)]. Averaging of ΘT_{UT} and ΘT_{TP} for 2 or more isobaric levels provides additional data smoothing and selection of the most stable spatial-temporal variations.

3.6. Calculation of integral indicators for anomalous variations in temperature time series

We converted the time series of ΘT_{UT} and ΘT_{TP} using the moving window, representing each point in the series as a variance of m previous values. The size of the "window" (m) was equal to 32 (4 days), which approximately corresponds to the high-frequency component in $T(t)$. Relatively fast, anomalous $[\Delta T(x_i, y_j, n, t, p_k) > \sigma_T(x_i, y_j)]$ and correlated temperature variations were determined as a product of variances at selected isobaric levels:

$$D = D_{\Theta T}^{UT} \cdot D_{\Theta T}^{TP} \quad (2)$$

To reduce «false» (in-phase) anomalies exceeding 2σ , we calculated D_{CORR} , taking into account correlation (R) between temperatures at UTLS levels under consideration. We calculated the integral index D_{CORR} as



Figs. 3(a-h). Temperature time series, T_1 (350 hPa) and T_2 (100 hPa) (a), wavelet scalograms (b, c), correlation coefficient (d), anomalies (e) and their moving variances (f), D and D_{corr} parameters (g), magnitude (M) and number of earthquakes per day N_{events} (h) during the period from 15 October to 15 December, 2015 (Seismic event 17 November, 2015; $M = 5.8$)

following : $D_{\text{corr}} = 0$, if $R \geq 0$ and $D_{\text{corr}} = D \times |R|$, if $R < 0$. That is, D_{corr} is equal to zero at positive correlation and is adjusted, depending on R value in antiphase temperature changes.

3.7. Determination of spatial-temporal distribution of D_{corr} parameter

We calculate and visualize D (D_{corr}) integral parameter in one-dimensional and two-dimensional representation. For each coordinate point of the region of interest and every 3 hour we calculated the following parameters: $\langle T(p_k) \rangle$, σ_T , ΘT , D , R , D_{corr} . Then we constructed contour maps of spatial distribution of D_{corr} and plotted epicenters of the seismic events.

3.8. Analysis of temperature and seismic data

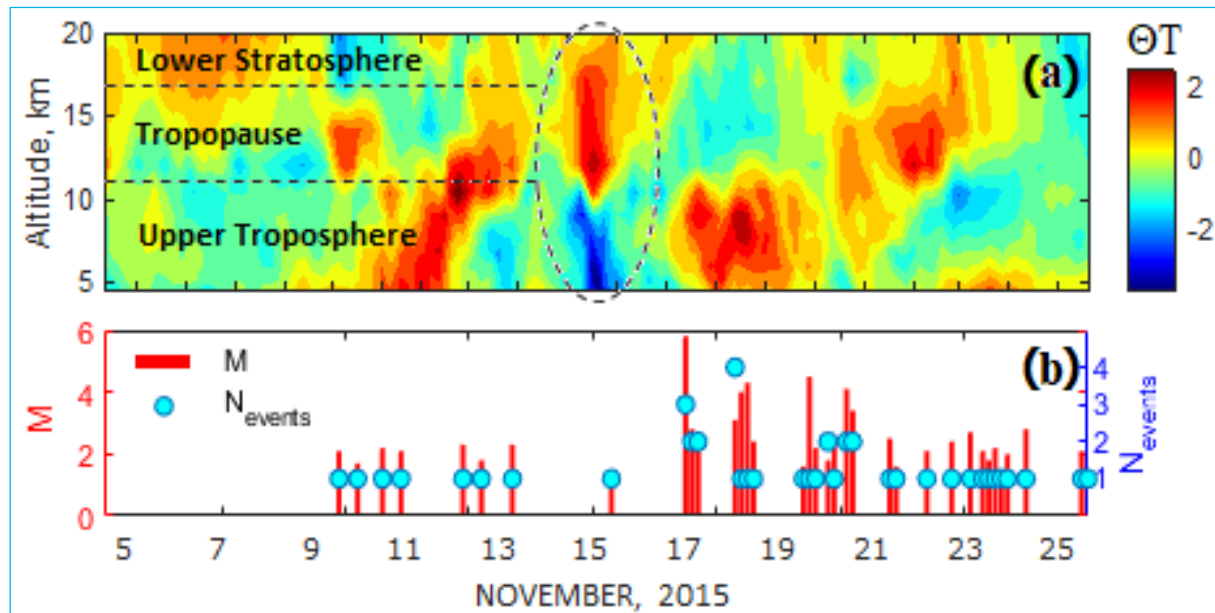
These maps make it possible to trace the dynamics of spatial-temporal changes of D_{corr} , in particular, during the period prior to major earthquakes and to select regions and moments of anomalous temperature changes. D_{corr} values exceeding 1 indicates anomalous and antiphase short-time temperature variations in both atmospheric layers and possible seismicity activation.

4. Temperature variations and seismic data analysis

4.1. Anomalies in UTLS temperature time series over the area of strong earthquakes preparation

We analyzed satellite data to examine temperature variability before, during and after the earthquakes. It is important to not only highlight common features but also distinguishing features of atmospheric effects associated with particular seismic events. We analyzed the temperature time series averaged over the area $\pm 1^\circ$ near the earthquake epicenters, which corresponds to sizes of preparation areas of strong seismic events discussed, for example, in Pavlidou *et al.*, 2019.

Figs. 3(a-h) illustrates an example of the processing of temperature time series, corresponding to seismic activation and the main event with magnitude $M = 5.8$, registered on 17th November, 2015 (the time range is 15 October - 15 December, 2015). The plots illustrate all the stages of workflow : average ΘT_{UT} and ΘT_{TP} at 350 and 100 hPa levels [Fig. 3(a)], wavelet spectrograms [Figs. 3(b&c)], correlation coefficient [Fig. 3(d)], temperature anomalies [Fig. 3(e)], sliding variances [Fig. 3(f)] and their product (D and D_{corr}) [Fig. 3(g)], correlating with seismicity [Fig. 3(h)] and indicating sharp temperature changes prior to main seismic event.



Figs. 4(a&b). Altitude-temporal distribution of atmospheric temperature anomalies (ΘT) in UTLS over the epicenter of the earthquake $M = 5.8$ (17 November, 2015) (a) magnitudes (M) and number of earthquakes per day N_{events} and (b) during the period 5-25 November, 2015

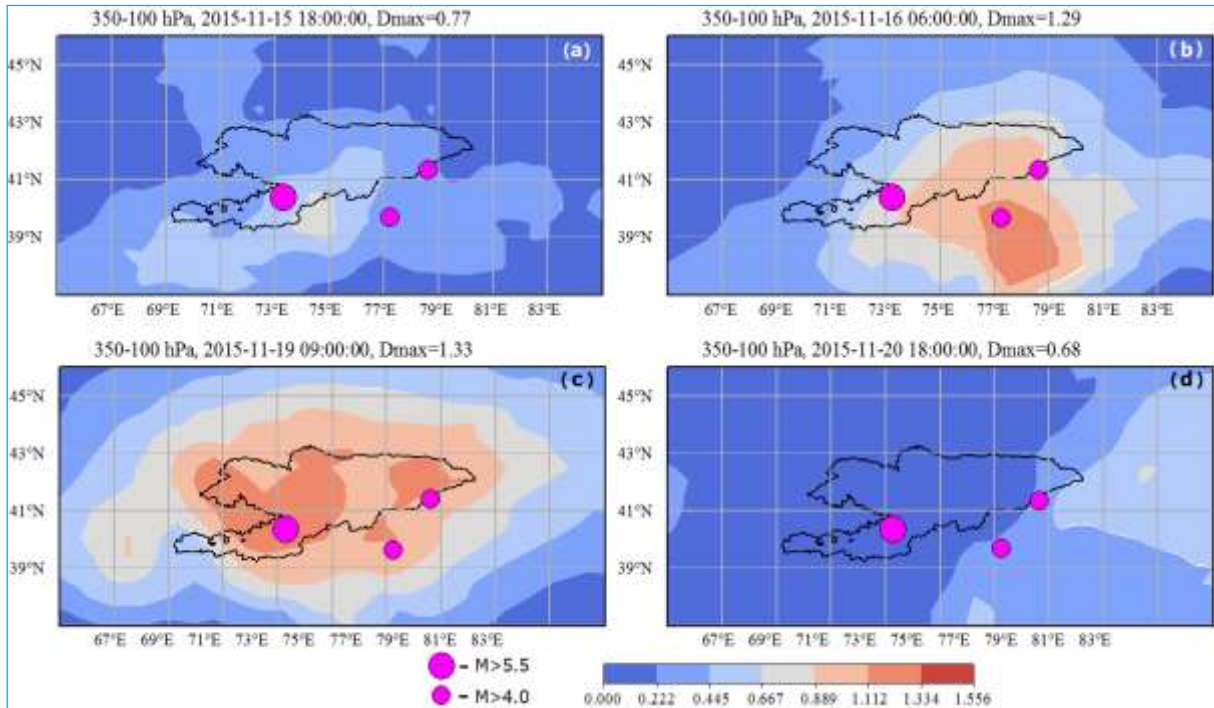
We can observe the following features in temperature variations as reaching the moment of the earthquake: reduction (destruction) in synoptic scale oscillations (Seidel, 2006) with a period of ~ 10 -11 days and noticeable increase in 4-6 days period band [Figs. 3(b&c)] and increasing in variance [Fig. 3(f)]. Increase of D_{CORR} can be explained as simultaneous presence of two interrelating factors - increase of amplitudes of short-time variations above and under the tropopause and the antiphase nature of these changes. It is clear that high values of D_{CORR} , notably exceeding background values ($D_{\text{CORR}} > 1.0$) and indicating anomalous changes in the thermal structures of the upper troposphere/lower stratosphere, were observed approximately 2 days before earthquake with magnitude $M = 5.8$. The more intensive second peak of D_{CORR} coincided in time with earthquake $M = 4.3$ (19 November 2015; 00:00:41 UTC).

Fig. 4(a) presents 20-day fragment of altitude-temporal section of ΘT , showing formation of a negative temperature anomaly in the upper troposphere ΘT_{UT} (~ 6.0 -9.0 km or 400-300 hPa) and a positive anomaly in the tropopause ΘT_{TP} (~ 12.0 -17.5 km or 200-100 hPa), exceeding 2σ and characterized by synchronous antiphase changes preceding a strong earthquake [Fig. 4(b)]. The dynamic process in the upper troposphere, which started several days before the earthquake (10-11 November, 2015), was characterized by transfer of energy upwards (ascending heat flux) to the tropopause level.

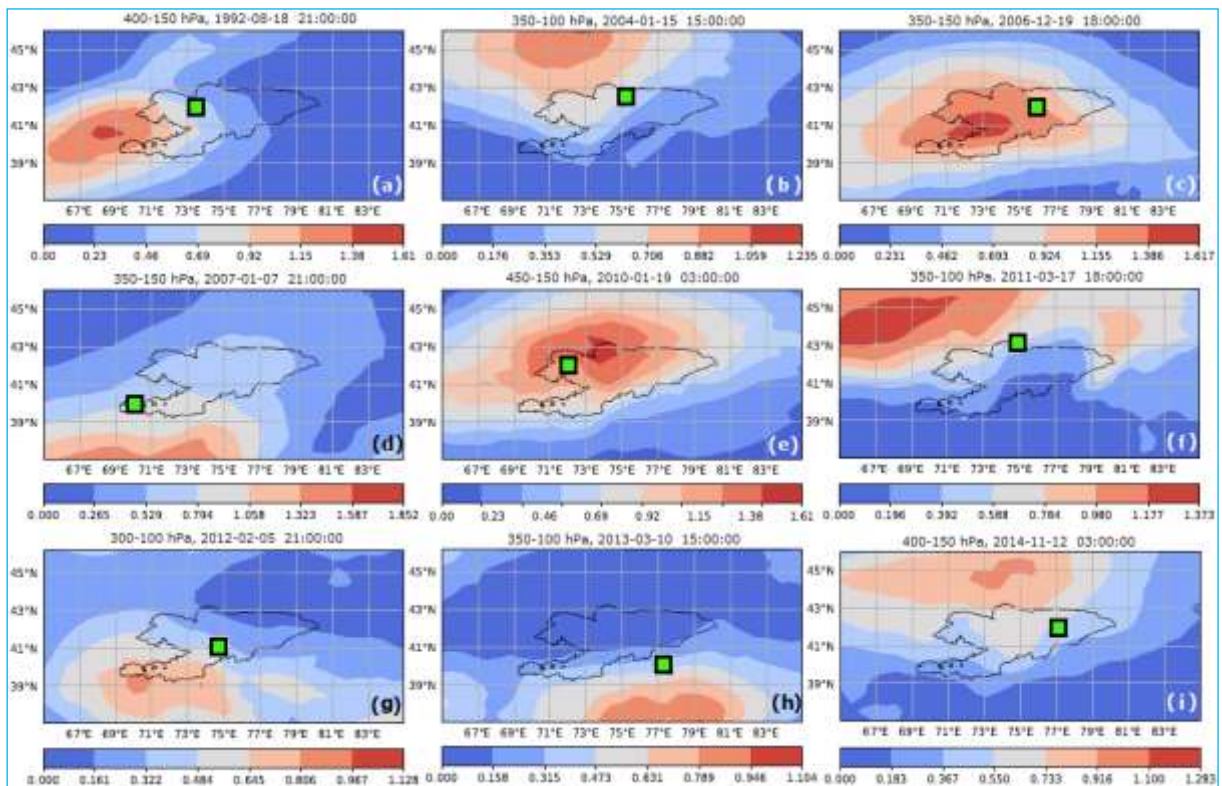
4.2. Spatial-temporal distribution of anomalous temperature perturbations in the tropopause

Figs. 5(a-d) show spatial-temporal distribution of anomalous temperature perturbations based on satellite data. The maps demonstrate dynamics of temperature anomaly development during the period of 15-20 November, 2015, when the earthquakes $M = 5.8$ (17 November, 2015; 17:29:37 UTC), $M = 4.0$ (18 November, 2015; 20:54:35 UTC) and $M = 4.3$ (19 November, 2015; 00:00:41 UTC) were registered. Formation of high D_{CORR} values was synchronized in both time and space with seismic activity in the region and was localized in the space, having horizontal scales of several hundred kilometers [Figs. 5(b&c)]. We should also note a formation of strong post-seismic temperature anomalies ($D_{\text{CORR}} = 1.2$ -1.3), located in the immediate vicinity of earthquake epicenters [Fig. 5(c)]. The anomalous temperature variations over epicentral area were of short duration (from several hours to 1-2 days), but the most important thing is that they were accurately synchronized with seismic activity, being prior to the strongest seismic shocks [Figs. 3(g) & 5(b)]. The most significant change of D_{CORR} took place several days before the earthquake.

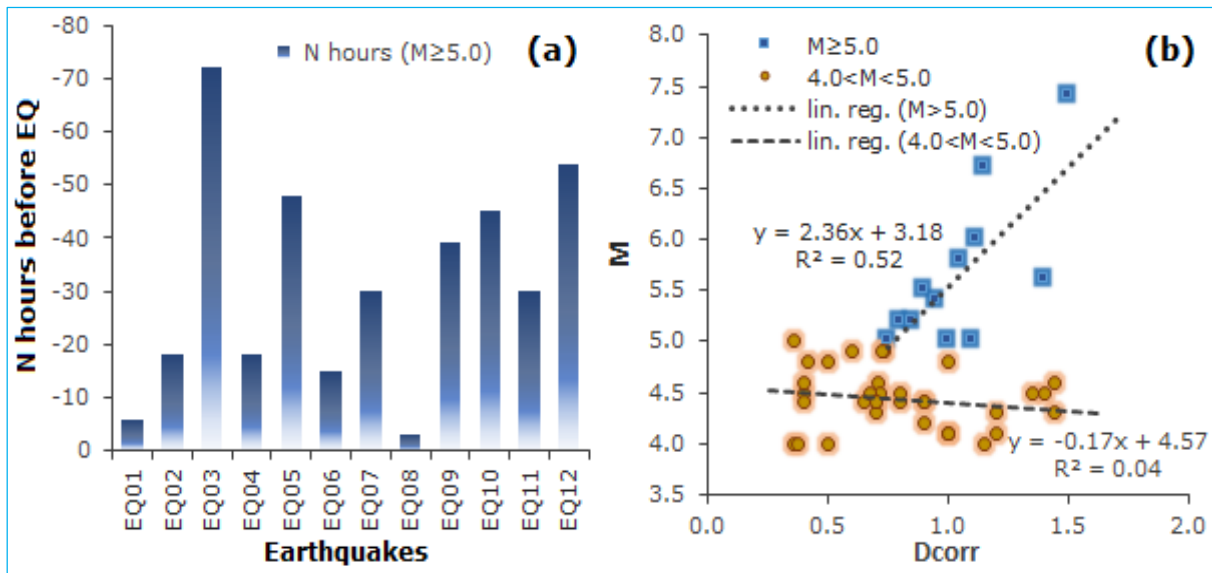
High correlation between earthquake moment and detected anomalous temperature changes in the upper troposphere / lower stratosphere appeared in all cases of strong earthquakes in the Northern and Central



Figs. 5(a-d). Evolution of spatial distribution of D_{CORR} integral parameter during preparation and occurrence of earthquakes $M = 5.8$ (17 November, 2015), $M = 4.0$ (18 November, 2015) and $M = 4.3$ (19 November, 2015)



Figs. 6(a-i). Spatial distribution of D_{CORR} during the period of preparation of earthquakes $M > 5.0$: EQ01 (a), EQ02 (b), EQ03 (c), EQ04 (d), EQ06 (e), EQ07 (f), EQ08 (g), EQ09 (h), EQ10 (i), (See Table 1)



Figs. 7(a&b). The time delay between temperature anomalies over the epicentral area and seismic events EQ01–EQ12 (a) correlation between D_{CORR} and the earthquake magnitude $M \geq 5.0$ and $4.0 < M < 5.0$ (b)

Tien-Shan selected for analysis [Figs. 6(a-i)]. The common characteristic of all the events presented on the maps is increase in values of D_{CORR} , which may be interpreted as a possible indicator of seismic activity.

At the same time, antiphase anomalous temperature perturbations in the tropopause characterized by high D_{CORR} may be also considered as triggers of seismic events, which are able to accelerate earthquakes imminent in the Earth crust regardless of atmospheric processes (Adushkin *et al.*, 2008).

The main differences between considered periods of preparation of the earthquakes, occurred within the same area were the delay (from ~3 to 72 hours) between the seismic events, the temperature anomaly over the epicentral area [Fig. 7(a)] and spread between D_{CORR} maximum values. Preliminary analysis of the results showed a moderate correlation ($R \sim 0.7$) between D_{CORR} and the earthquake magnitude $M \geq 5.0$ [Fig. 7(b)]. As for earthquakes with $4.0 < M < 5.0$, approximately 50% (30 of 58) of temperature anomalies were not detected within the 72-hour time interval.

As the all points in D_{CORR} plots and distribution maps are in fact forecasting and are based on temperature changes during the period prior to the earthquake, such synchronization in time of temperature anomalies and strong seismic events may mean a certain generality of physical processes taking place at that time.

5. Conclusions

In this paper, we presented results of analysis of earthquakes with magnitudes from 5.0 to 7.4 in the territory Kyrgyzstan or near its borders during the 1992–2015 period, obtained using algorithms for satellite data processing. The algorithms allow diagnosing short-time anomalous changes in spatial-temporal distribution of temperature, which precede strong earthquakes. We considered opposite in sign anomalous changes of temperature amplitude, located below and above the tropopause as the main features characterizing atmospheric temperature prior to strong earthquakes. The anomalous temperature perturbations with horizontal scales of several hundred kilometers were observed in all the considered cases for the periods not exceeding 3 days before the main seismic event.

The obtained results allow us to assume that temperature anomalies may be considered as dynamic perturbation in the upper troposphere / lower stratosphere. We assume that horizontal (advective) movements of air masses play an important role in the development of temperature perturbations, which appear directly prior to a seismic event, dominating over the other factors (*e.g.*, convective transfer of heat energy, gravity waves).

We should note the versatility of the developed algorithms, which allows analyzing various types of experimental data.

Acknowledgements

The authors are grateful to Giovanni team of NASA GES DISC for free access to satellite measurement data.

The study is partially performed within the framework of the state task of the Federal State Budgetary Institution of Science, Research Station of Russian Academy of Sciences in Bishkek (theme No. AAAA-A19-119020190064-9).

The contents and views expressed in this research paper are the views of the authors and do not necessarily reflect the views of the organizations they belong to.

References

- Adushkin, V. V., Loktev, D. N. and Spivak, A. A., 2008, "The effect of baric disturbances in the atmosphere on microseismic processes in the crust", *Izvestiya. Physics of the Solid Earth*, **44**, 6, 510-517.
- Birner, T., 2006, "Fine-scale structure of the extratropical tropopause region", *J. Geophys. Res.*, **111**, D04104, doi: 10.1029/2005JD006301.
- Donoho, D. L. and Johnstone, J. M., 1994, "Ideal spatial adaptation by wavelet shrinkage", *Biometrika*, **81**, 3, 425-455.
- Gadre, V. M., Dimri, V. M. and Chandrasekhar, E., 2014, "Wavelets and fractals in earth system sciences", *Boca Raton, FL: Taylor & Francis Inc.*, p286.
- Jiao, Z. H., Zhao, J. and Shan, X., 2018, "Pre-seismic anomalies from optical satellite observations: A review", *Nat. Hazards Earth Syst. Sci.*, **18**, 4, 1013-1036.
- Kashkin, V. B., 2013, "Inner gravity waves in the troposphere", *Atmospheric and Oceanic Optics*, **26**, 10, 908-916.
- Kashkin, V. B., Romanov, A. A., Grigoriev, A. S. and Baskova, A. A., 2012, "Troposphere Effects of Tuva Earthquakes Detected with Space Technology", *J. Sib. Fed. Univ. Eng. Technol.*, **5**, 2, 220-228.
- Kashkin, V., Sverdlik, L., Odintsov, R., Rubleva, T., Simonov, K., Romanov, A. and Imashev, S., 2020, "Features of atmospheric disturbances in temperate latitudes before strong earthquakes (M>7) according to satellite measurements", *E3S Web of Conferences*, **149**, 03011 (2020), RPERS 2019.
- Manney, G. L., Hegglin, M. I., Lawrence, Z. D., Wargan, K., Millán, L. F., Schwartz, M. J., Santee, M. L., Lambert, A., Pawson, S., Knosp, B. W., Fuller, R. A. and Daffer, W. H., 2017, "Reanalysis comparisons of upper tropospheric-lower stratospheric jets and multiple tropopauses", *Atmos. Chem. Phys.*, **17**, 11541-11566.
- Morozova, A. L., Blanco, J. J. and Ribeiro, P., 2017, "Modes of temperature and pressure variability in midlatitude troposphere and lower stratosphere in relation to cosmic ray variations", *Space Weather*, **15**, 673-690.
- Ouzounov, D., Pulinets, S., Hattori, K. and Taylor, P., 2019, "Pre-Earthquake Processes: A Multidisciplinary Approach to Earthquake Prediction Studies", *AGU*, p384.
- Pavlidou, E., Van Der Meijde, M., Van Der Werff, H. and Hecker, C., 2019, "Time Series Analysis of Land Surface Temperatures in 20 Earthquake Cases Worldwide", *Remote Sens.*, **11**, 1, 61, doi:10.3390/rs11010061.
- Pergola, N., Aliano, C., Coviello, I., Filizzola, C., Genzano, N., Lacava, T., Lisi, M., Mazzeo, G. and Tramutoli, V., 2010, "Using RST approach and EOS-MODIS radiances for monitoring seismically active regions: a study on the 6 April 2009 Abruzzo earthquake", *Nat. Hazards Earth Syst. Sci.*, **10**, 239-249.
- Pilch, Kedzierski R., Matthes, K. and Bumke, K., 2017, "Wave modulation of the extratropical tropopause inversion layer", *Atmos. Chem. Phys.*, **17**, 4093-4114.
- Prakash, R. and Srivastava, H. N., 2015, "Thermal anomalies in relation to earthquakes in India and its neighbourhood", *Current Science*, **108**, 11, 2071-2082.
- Pulinets, S. A., Morozova, L. I. and Yudin, I. A., 2014, "Synchronization of atmospheric indicators at the last stage of earthquake preparation cycle", *Res. Geophys.*, **4**, 1, 45-50.
- Randel, W. J., Seidel, D. J. and Pan, L. L., 2007, "Observational characteristics of double tropopauses", *J. Geophys. Res.*, **112**, D07309, doi:10.1029/2006JD007904.
- Sanchez-Dulcet, F., Rodríguez-Bouza, M., Silva, H. G., Herraiz, M., Bezzeghoud, M. and Biagi, P. F., 2015, "Analysis of observations backing up the existence of VLF and ionospheric TEC anomalies before the Mw 6.1 earthquake in Greece, January 26, 2014", *J. Phys. Chem. Earth.*, **85-86**, 150-166.
- Seidel, D. J. and Randel, W. J., 2006, "Variability and trends in the global tropopause estimated from radiosonde data", *J. Geophys. Res.*, **111**, D21101, doi:10.1029/2006JD007363.
- Sverdlik, L. G. and Imashev, S. A., 2018, "Diagnosis of Atmospheric Temperature Anomalies in Seismically Active Regions of Asia on the Basis of Satellite Data", *J. Sib. Fed. Univ. Eng. Technol.*, **11**, 8, 956-963.
- Sverdlik, L., Imashev, S. and Yamskikh, T., 2019, "Anomalous atmospheric temperature perturbations over seismically active regions of Europe according to satellite measurements", *E3S Web of Conferences*, **75**, 02004 (2019), RPERS 2018.
- Tramutoli, V., Di Bello, G., Pergola, N. and Piscitelli, S., 2001, "Robust satellite techniques for remote sensing of seismically active areas", *Ann. Geophys-Italy*, **44**, 2, 295-312.

- Tramutoli, V., Marchese, F., Falconieri, A., Filizzola, C., Genzano, N., Hattori, K., Lisi, M., Liu, J. Y., Ouzounov, D., Parrot, M., Pergola, N. and Pulinets, S., 2019, "Tropospheric and Ionospheric Anomalies Induced by Volcanic and Saharan Dust Events as Part of Geosphere Interaction Phenomena", *Geosciences*, **9**, 4, 1-26.
- Tronin, A., 2010, "Satellite remote sensing in seismology : A review", *Remote Sens.*, **2**, 1, 124-150.
- Yadav, K. S. and Pathak, J. S., 2018, "Anomalous variation in GPS based Total Electron Content (TEC), prior to six (6) earthquakes in 2016", *Mausam*, **69**, 3, 419-426.
- Zhang, Y. and Meng, Q., 2019, "A statistical analysis of TIR anomalies extracted by RSTs in relation to an earthquake in the Sichuan area using MODIS LST data", *Nat. Hazards Earth Syst. Sci.*, **19**, 535-549.
-